Reac Kinet Mech Cat (2017) 121:17–29
DOI 10.1007/s11144-016-1123-5

Heterogeneous catalytic Wacker oxidation of ethylene over oxide-supported Pd/VO_x catalysts: the support effect

Róbert Barthos[1] · Gyula Novodárszki[1] · József Valyon[1]

Received: 14 November 2016 / Accepted: 15 December 2016 / Published online: 22 December 2016
© Akadémiai Kiadó, Budapest, Hungary 2016

Abstract This paper concerns the selective oxidation of ethylene (EE) to acetaldehyde (AL) and acetic acid (AA) by oxygen in the presence of steam over non-supported Pd/V_2O_5 catalyst and over Pd/V_2O_5 catalysts supported by SiO_2, TiO_2, γ-Al_2O_3, and α-Al_2O_3. A flow-through microreactor was applied at atmospheric pressure in the temperature range of 150–200 °C. The WHSV of EE was 0.17 or 0.84 h^{-1}. The vanadia content of the supported catalysts was 17 wt%, whereas their Pd content was 0.8 wt%. The reducibility of vanadia was determined using temperature-programmed reduction by hydrogen (H_2-TPR). Applying ultraviolet–visible (UV–Vis) spectroscopy and X-ray diffractometry (XRD), different vanadia species were identified over different supports. In the Pd/V_2O_5/α-Al_2O_3 catalyst, the vanadia had the same structure as in the Pd/V_2O_5 preparation. Even the low surface area α-Al_2O_3 support affects the Wacker oxidation activity of the catalyst. Vanadia deposited on the surface of TiO_2 or γ-Al_2O_3 forms easily reducible polymeric species. In interaction with Pd, this polymeric species is responsible for the total oxidation EE to CO_2. Palladium, bound to the surface of bulk V_2O_5 or to monomeric vanadate-like species on silica, forms Pd/VO_x redox pairs, which are active and selective catalytic centers of the Wacker reaction. The Wacker mechanism was verified by test reactions, where one of the four components, such as Pd, V_2O_5, O_2, or H_2O, was left out of the reacting system. In the absence of any of the

✉ Róbert Barthos
barthos.robert@ttk.mta.hu

Gyula Novodárszki
gyula.novodarszki@ttk.mta.hu

József Valyon
valyon.jozsef@ttk.mta.hu

[1] Institute of Materials and Environmental Chemistry, Research Centre for Natural Sciences, Hungarian Academy of Sciences, Magyar Tudósok Körútja 2, Budapest 1117, Hungary

components, no selective catalytic partial EE oxidation proceeded, indicating that the Wacker mechanism could not operate.

Keywords Ethylene oxidation · Wacker mechanism · Supported Pd/VO_x catalysts · UV–vis spectroscopy · H_2-TPR

Introduction

Oxidative dehydrogenation of ethane is a rapidly growing technology of ethylene (EE) production. Due to phasing out of the naphtha pyrolysis technology of EE production, where 1,3-butadiene (BD) was obtained as by-product, a need is emerging for alternative BD production technologies. Ethylene is a plausible raw material of BD production. It has been known for long that BD can be obtained by the catalytic conversion of ethanol (EL) or preferably by reacting EL and acetaldehyde (AL). Ethanol can be obtained from EE by catalytic hydration [1]. Biomass-derived ethanol can also be used [2, 3]. To obtain AL from EE, selective catalytic oxidation must be carried out. The expectedly growing demand for AL motivated us to study the heterogeneous catalytic selective EE oxidation to AL.

Two technologies were developed for the production of BD from EL. In the Lebedev process [4], EL is converted to BD over mixed oxide catalyst, like MgO/SiO_2 or ZnO/Al_2O_3. The first step of obtaining BD from EL is dehydrogenation of EL to obtain AL. The reaction proceeds then through consecutive reactions, such as aldol addition, dehydration, and hydrogenation, to get intermediates, 3-hydroxybutanal, crotonaldehyde, and crotyl alcohol, and, as a final step, dehydration of crotyl alcohol to get 1,3-BD. The hydrogenation of crotonaldehyde intermediate to alcohol can occur in the reaction mixture through transfer hydrogenation by EL.

In another technology, known as the Ostromislensky process [5], a mixture of EL and AL is converted over alumina or clay catalyst. This technology applies two sequential catalytic reactors. In the first reactor, EL is dehydrogenated to AL, whereas in the second one the produced AL reacts with co-fed EL to form BD.

Several studies revealed [6, 7] that a higher yield of BD was obtained from a feed of AL/EL mixture than from pure EL. Therefore, there is an obvious interest to get AL from the readily available EE. Niiyama et al. [6] showed that AL could not be converted into BD over SiO_2/MgO catalyst at all. Under the same reaction conditions, the conversion of pure EL and 10 vol% AL/EL mixture to BD were 10 and 30%, respectively. The reaction was also studied over ZrO_2/SiO_2 and Ta_2O_5/SiO_2 catalysts [7, 8]. At a somewhat higher AL content of the feed, the molar conversion of the AL/EL mixture was near to 30–40%, whereas the BD yield was also about 20–30%. From ethanol only, under the same reaction conditions, only EE and diethyl ether were obtained.

The discussion above suggest that besides processing bioethanol the processing of cheap EE is an alternative route of BD production. The raw material EE can be hydrated to EL in one reactor, partially oxidized to AL in another reactor, and EL and AL is mixed and converted to BD in a third reactor.

The heterogeneous catalytic hydration of EE to EL is a well-known acid catalyzed process [9]. Since 1960, the Wacker process is prevailing for the catalytic oxidation of EE to AL [10].

The Wacker process realizes the aqueous-phase oxidation of EE by dioxygen in the presence of HCl, $PdCl_2$ and $CuCl_2$. The catalytic cycle rests on the cooperation of Pd^{2+}/Pd^0 and Cu^{2+}/Cu^+ redox couples. During the oxidation of EE, Pd^{2+} is reduced to Pd^0, which is reoxidized to Pd^{2+} by Cu^{2+} and, at the end of a cycle, gaseous oxygen oxidizes the formed Cu^+ to Cu^{2+}. Generally, the industrial application of homogeneous catalytic reactions involves the disadvantage of complicated separation of product and catalyst and the moderate stability of the catalyst under severe reaction conditions. However, these problems can be overcome by immobilizing homogeneous catalysts on the surface of solid support. The present paper relates to the formation of AL from EE by realizing the Wacker process on a heterogeneous catalytic route.

Previous results showed that Wacker oxidation could be heterogenized by the combination of palladium with a solid, which is capable of re-oxidizing Pd^0 to Pd^{2+}. The best results were achieved by using copper [11, 12] and vanadium [13, 14] supported on different materials (zeolites [11], clays [12], oxides [13, 14], activated carbons [15] etc.). Li et al. [14] compared the catalytic performance of Pd/V_2O_5 redox-pair on different supports (SiO_2, TiO_2 and γ-Al_2O_3) at 190 °C in the conversion of propylene to acetone and found that the titania-supported catalyst was the most active. Stobbe-Kreemers [13] reported that the TiO_2 supported Pd/V_2O_5 catalysts show an order of magnitude higher activity than the catalysts based on γ-Al_2O_3. In early studies, Seoane et al. [16] proved that Pd, supported on crystalline V_2O_5 also can convert EE to AL.

This study concerns the preparation, characterization, and catalytic testing of different oxide-supported Pd/V_2O_5 catalysts. The oxide support was shown to affect both Wacker activity and selectivity of catalyst.

Experimental

Catalyst preparation

Supports as γ-Al_2O_3 (Ketjen CK 300, Akzo-Chemie, specific surface area, SSA = 190 m^2/g), α-Al_2O_3 (prepared from γ-Al_2O_3 by calcination at 1200 °C for 4 h, SSA = 2 m^2/g), SiO_2 (Cab–O–Sil, M-5, Cabot GmbH, Hanau SSA = 197 m^2/g), and TiO_2 (Aeroxide TiO_2, P-25, Evonik Industries AG, SSA = 55 m^2/g) were impregnated by a decavanadate ($V_{10}O_{56}^{6-}$) solution. The solution was prepared from metavanadate solution. Ten grams of ammonium metavanadate (NH_4VO_3, VEB Laborchemie, Apolda, 99.0% purity) was dissolved in 1 dm^3 distilled water and, in order to obtain decavanadate ions, the pH of the solution was adjusted to pH 4 by the stepwise addition of 0.1 mol/dm^3 HNO_3 solution. The impregnated supports were calcined at 400 °C for 4 h to obtain catalysts containing 17 wt % V_2O_5. An aliquot fraction of each supported vanadia sample was impregnated by $Pd(NH_3)_4(NO_3)_2$ (5.0 wt% Pd as solution, Strem Chemicals Inc.) solution and air-calcined again at

400 °C for 4 h. The Pd/V_2O_5 sample was prepared by one-step impregnation of commercial V_2O_5 (Sigma-Aldrich, 99.6 + %, metals basis). All the samples were impregnated by an amount of Pd solution to get catalyst, having Pd content of 0.8 wt%.

Characterization of catalysts

Specific surface area

Specific surface area (SSA) of the catalysts was obtained by the BET method from N_2 adsorption isotherm determined at −195 °C using a Quantachrome NOVA automated gas sorption instrument. Before measuring adsorption isotherms, the samples were outgassed by vacuum at 150 °C for 24 h.

X-ray powder diffraction

X-ray patterns were recorded by Philips PW 1810/3710 diffractometer applying monochromatized Cu K_α radiation (40 kV, 35 mA). The patterns were recorded at ambient conditions between 3° and 65° 2Θ, in 0.02° steps, counting in each step for 0.5 s.

Temperature-programmed reduction by hydrogen (H_2-TPR)

A flow-through microreactor made of quartz tube (I.D. 4 mm) was used. About 20 mg of catalyst sample (particle size: 0.63–1.00 mm) was placed into the reactor and was treated before the measurement in a 30 cm^3/min flow of O_2 at 400 °C for 1 h. Then the sample was cooled to room temperature in O_2 flow, flushed for 30 min by N_2 and contacted then with a 30 cm^3/min flow of 10% H_2/N_2 mixture. The reactor temperature was ramped up at a rate of 10 °C/min to 600 °C and kept at this temperature for 1 h while the effluent gas was passed through a trap, cooled by liquid nitrogen, and a thermal conductivity detector (TCD). Data were collected and processed by a computer. The hydrogen consumption was calculated from the area under the H_2-TPR curve. The system was calibrated by determining the H_2-TPR curve of CuO reference material.

UV–vis DRS spectroscopy

The in situ UV–vis DRS spectra were collected by Thermo Scientific Evolution 300 UV–vis spectrophotometer equipped with a Praying Mantis diffuse reflectance accessory and high temperature and pressure reaction chamber. The finely ground reference ($NaVO_3$, 99.9%, Na_3VO_4 99.98%, V_2O_5, 99.6 + %, Aldrich products) and catalyst samples were diluted with $BaSO_4$ (Alfa Aesar, Puratronic 99.998%) in an amount to fit the Kubelka–Munk function $F(R_\infty) < 1$ and measured against Spectralon as the background. In order to obtain the spectra of the dehydrated samples, the absorbance data were collected at 400 °C after in situ calcination at 400 °C in flowing oxygen for 30 min. The edge energies (E_g) for allowed transitions

were determined by finding the intercept of the straight line fitted to the low energy rise of the plot of $[F(R_\infty)h\nu]^2$ against $h\nu$ [17].

Catalytic activity measurements

Catalytic test reactions were carried out at atmospheric pressure in a fixed-bed, continuous flow tubular microreactor. Prior to the reaction, the catalysts were activated in oxygen flow (20 cm^3/min) for 1 h at 350 °C. The same treatment was applied to re-activate used catalysts. In the catalytic test, $C_2H_4/O_2/H_2O$/He gas mixture was fed on 500 mg of catalyst sample (particle size 0.63–1.00 mm). The partial pressures of EE, oxygen, and water were 3.4, 13.5, and 27 kPa. The effect of the partial pressures on the activity was studied by varying the partial pressure of oxygen and water in the ranges of 0–41 and 0–54 kPa on expense of the partial pressure of the helium. In the measurements of partial pressure dependence 100 mg of catalyst diluted with 400 mg of inert γ-Al_2O_3 was used. The total flow rate of the reaction mixture was always 30 cm^3/min. All gas lines of the apparatus were heated to 120 °C in order to avoid the condensation of water and reaction products. The reaction products were analyzed on-line by a Shimadzu GC-2010 gas chromatograph (GC) equipped with a 30-m HP-PLOT-U column, thermal conductivity and flame ionization detectors (TCD and FID). The calibration of the GC for each reactant and product compound was carried out separately. The conversion of EE was calculated from the EE concentrations in the feed and effluent. Selectivities were calculated from the molar product composition.

Results and discussion

The Wacker oxidation requires co-operation of Pd/VO_x catalyst/co-catalyst redox pair. It was proven using D_2O and H_2O^{18} water in the reaction mixture that oxygen atoms in the product AL originated from the water [18, 19]. The absence of V_2O_5, Pd, oxygen or water in the reacting system makes it obvious that simultaneous presence of each component is a must to initiate Wacker reaction (Fig. 1). Fig. 1a shows that without V_2O_5 in the supported catalyst, total oxidation is the dominant reaction even at temperature as low as at 150 °C. The formation of methane in traces and deactivation of the catalyst were also observed. In the absence of Pd, the EE conversion began at 225 °C and the only reaction product was again CO_2 (Fig. 1b). The role of oxygen in the Wacker oxidation reaction cycle is the selective re-oxidation of the co-catalyst, i.e. the reduced vanadium atoms. Fig. 2c shows that AL is formed with a selectivity close to 100% with low and constantly decreasing conversion even in the absence of oxygen. In the latter experiment, the V_2O_5 content of the catalyst was 2.78 mmol, while the amount of formed AL, determined by the integration of its formation rate curve versus reaction time, was 2.27 mmol. This observation indicates that V_2O_5 is able to re-oxidize Pd until reaching oxidation state V^{4+}, and that the reaction terminates when the co-catalyst loses its oxidation capacity. In the absence of water in the feed (Fig. 2d), in addition to CO_2, partially oxidized products (acetaldehyde and acetic acid) were formed, suggesting

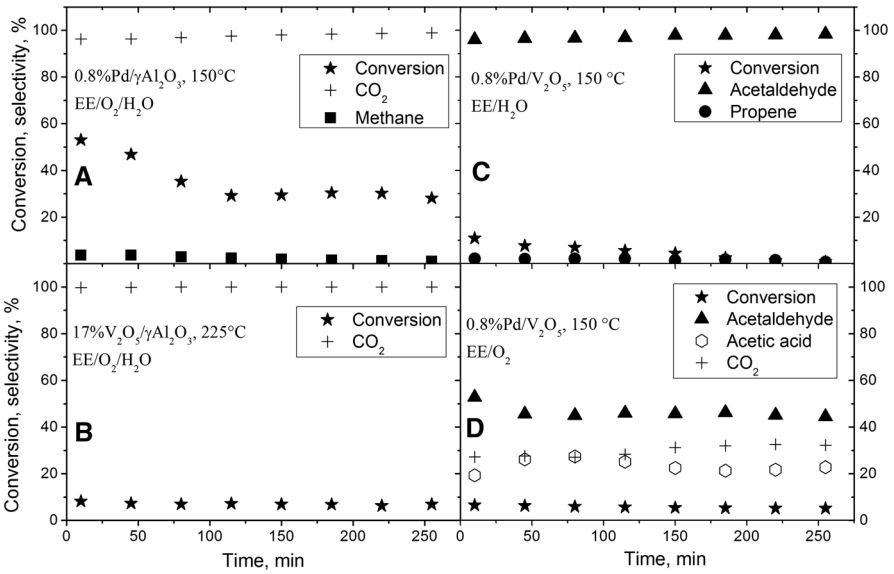

Fig. 1 Verification of the Wacker mechanism. In the absence of **a** V_2O_5, **b** Pd, or **c** O_2, and **d** H_2O, total oxidation or negligible conversion ethylene occurs

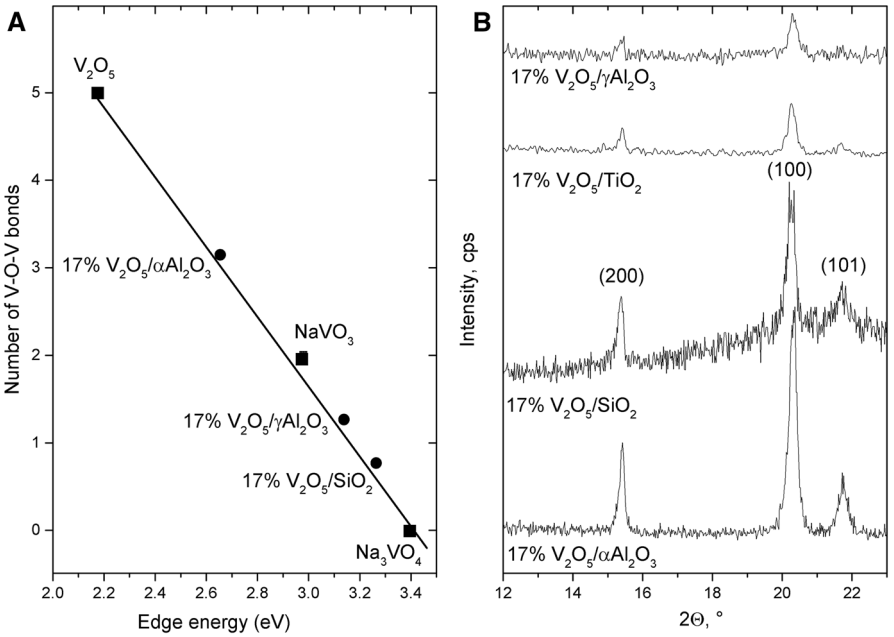

Fig. 2 **a** Plot of edge energy versus number of V–O–V bonds of vanadium atoms obtained by UV–vis DRS for vanadia compounds and catalyst samples, and **b** XRD patterns showing the most intense vanadia reflections of the catalyst samples

the appearance of some Wacker-type activity. However, the conversion was very low (vide infra). The presence of some water formed in the system by EE oxidation explains the appearance of Wacker oxidation.

Wachs and Weckhuysen [20] claimed that vanadia overlayer on oxide supports has a structure which is different from that of crystalline V_2O_5. Theoretical calculations based on the V–O bond lengths of crystalline V_2O_5 estimated monolayer surface vanadia coverage corresponding to a surface concentration of about 10 VO_x/nm^2 [21]. Indeed, the surface concentration, determined by Raman spectroscopy, was very similar for different oxide supports. It was 7.3 VO_x/nm^2 for Al_2O_3 and 7.9 VO_x/nm^2 for TiO_2 support [22]. The silica support, having a surface concentration as low as 0.7 VO_x/nm^2, was an exception. Over the SiO_2 support, bulk V_2O_5 crystals started to grow before monolayer coverage was achieved. In the present study, the same amount of V_2O_5 was impregnated on different supports. Because the surface area of the supports were different, the same amount of vanadia corresponded to different vanadia coverages (Table 1).

The DR UV–vis method is able to distinguish vanadia forms having different extents of polymerization [23]. The bulk orthovanadate (Na_3VO_4) contains isolated VO_4 units. In this structure, there are no vanadium atoms connected to another vanadium via oxygen (Fig. 2a). The metavanadate ($NaVO_3$) structure consists of polymeric VO_3 chains, where every vanadium atom is linked to two other one through oxygen atoms. In bulk V_2O_5, the number of V–O–V linkages is 5 for each vanadium atom. The E_g was found to be 2.18 eV for bulk V_2O_5, 2.98 eV for pure $NaVO_3$ and 3.40 eV for Na_3VO_4 (Fig. 2a). In a $V_2O_5/NaVO_3/Na_3VO_4$ mechanical mixture, each component contributed to the measured E_g value in proportion to its molar fraction in the mixture. This means that from the E_g edge energy of a supported vanadia catalyst, the percentage of isolated, polymeric and bulk vanadia forms can be estimated using an E_g versus composition calibration line. Based on the structural assignments of Gao and Wachs [23], the following surface vanadia structures were identified on the applied supports: (i) the SiO_2 ($E_g = 3.26$)

Table 1 Characterization of catalysts

Catalyst	Surface area (m^2/g)	XRD p.a[a]	Edge energy[b] (eV)	Vanadia coverage (V/nm^2)
$Pd/V_2O_5/SiO_2$[c]	159 (197)[d]	82	3.25	6.9
$Pd/V_2O_5/\gamma Al_2O_3$[c]	145 (190)[d]	20	3.12	7.1
$Pd/V_2O_5/TiO_2$[c]	45 (55)[d]	30	n.m.[d]	27.1
$Pd/V_2O_5/\alpha Al_2O_3$[c]	4 (2)[d]	230	2.62	67.8
Pd/V_2O_5[e]	8 (8)[d]	n.m.[f]	2.21.	–

[a] Peak area of the most intense V_2O_5 XRD line (001) Card N° 41-1426

[b] Edge energy of absorption peak determined by UV–vis DRS

[c] The supports were impregnated with 17 wt% V_2O_5 and 0.8 wt% Pd

[d] Surface area of pure supports

[e] 0.8 wt% Pd supported on pure V_2O_5

[f] Not measured

contained predominantly isolated VO_4 and a minor amount of bulk V_2O_5 phase, (ii) the γ-Al_2O_3 ($E_g = 3.14$) contained mixture of polymeric (VO_3) and isolated (VO_4) ($\sim$60 vs. 40%) vanadia, and traces of bulk V_2O_5, (iii) the α-Al_2O_3 ($E_g = 2.65$) contained mainly VO_5/VO_6 polymer with a minor amount VO_3 polymeric chain structure. The presence of V_2O_5 was detected by XRD (vide infra). Results of XRD and UV–vis measurements proved that vanadia coverage over γ-Al_2O_3 (7.1 V/nm^2) is close to monolayer.

The TiO_2 support exhibits strong absorption in the UV–vis region, which overwhelms the weaker absorption from the smaller amount of supported vanadium oxide species, thus no reliable results can be extracted from UV-DRS spectra of the titania supported vanadia samples [23]. However, the crystalline surface V_2O_5 species can be characterized by XRD (Fig. 2b). In accordance with the results of UV–vis measurements, the most intense and narrowest reflection of the V_2O_5/α-Al_2O_3 sample at 20.3° indicates the presence of large vanadia crystallites. Bulk V_2O_5 phase could be detected also in the V_2O_5/SiO_2 sample suggesting that the formation of V_2O_5 crystallites was more facile than the spreading of vanadia in monolayer. Over γ-Al_2O_3 and TiO_2, the growth of bulk phase just started to develop. These supports are covered with polymeric VO_3 species. However, the presence of isolated VO_4 could not be excluded.

Reducibility characterizes the co-catalytic activity of the VO_x component, i.e. the ability of the vanadia oxygen atoms to re-oxidize the Pd redox sites. H_2-TPR measurements were performed to characterize the reduction properties of supported VO_x and Pd/VO_x phases (Fig. 3). The H_2 consumptions, calculated from the

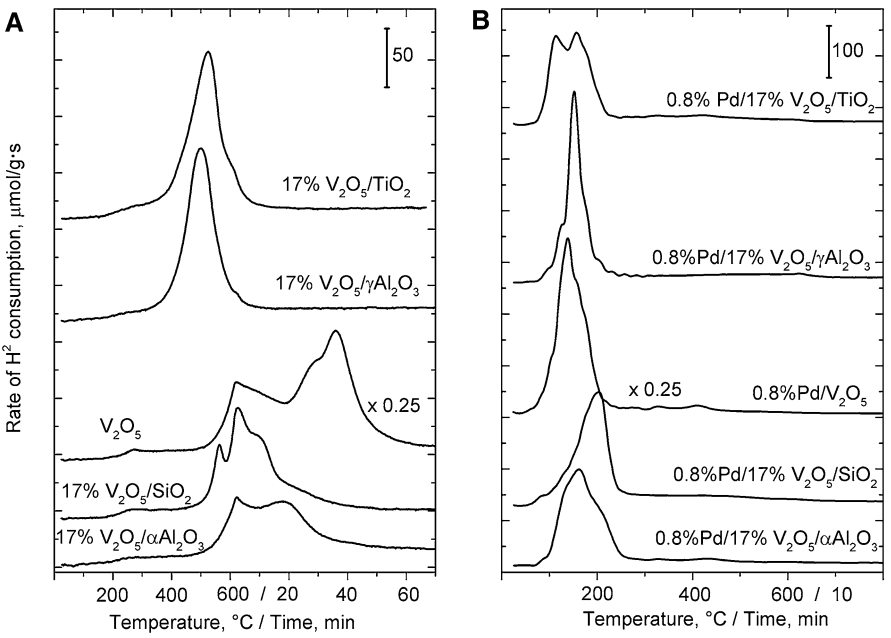

Fig. 3 H_2-TPR profiles of **a** supported V_2O_5 and **b** supported Pd/V_2O_5 catalysts

Table 2 Results of H_2-TPR measurements

Catalyst[a]	Low-temperature peak			High-temperature peak			$\Sigma H_2/V$
	H_2 (mmol/g)	T_{max} (°C)	H_2/V	H_2 (mmol/g)	T_{max} (°C)	H_2/V	
V_2O_5/TiO_2	–	–	–	2.16	524	1.15	1.15
$Pd/V_2O_5/TiO_2$	1.76	115	0.94	0.41	–	0.21	1.15
$V_2O_5/\gamma\text{-}Al_2O_3$	–	–	–	2.00	496	1.07	1.07
$Pd/V_2O_5/\gamma\text{-}Al_2O_3$	1.71	150	0.91	0.31	–	0.16	1.07
V_2O_5	–	–	–	11.72	600/36[b]	1.06	1.06
Pd/V_2O_5	9.95	132	0.81	1.08	–	0.09	0.90
V_2O_5/SiO_2	–	–	–	2.05	600/3[c]	1.09	1.09
$Pd/V_2O_5/SiO_2$	1.69	203	0.90	0.36	–	0.19	1.09
$V_2O_5/\alpha\text{-}Al_2O_3$	–	–	–	1.87	600/2[b]	1.00	1.00
$Pd/V_2O_5/\alpha\text{-}Al_2O_3$	1.83	163	0.97	0.20	–	0.10	1.07

Calculated from the results shown in Fig. 3

[a] The supports were impregnated with 17 wt% V_2O_5 and 0.8 wt% Pd

[b] Final temperature of the heating program/time in minutes on the temperature

integrated area of the H_2-TPR peaks, are listed in Table 2. It is known that the reduction of supported palladium oxide starts at around 0 °C [24]. The metallic palladium can then initialize hydrogen spill-over to the vanadia or to the support. In this process, hydrogen dissociates on the palladium and moves to the surface of the surrounding oxide lowering its oxidation state or forming bronze [25]. As a result, a reduction peak of V_2O_5 appears at much lower temperature than that for the Pd-free supported vanadia samples. Over Pd-free TiO_2 and $\gamma\text{-}Al_2O_3$, the reduction of vanadia starts at about 300 °C (Fig. 3a). Note that over these supports, the main vanadia form is close to monolayer thickness. The reduction of bulk V_2O_5 and supported bulk vanadia species over $\alpha\text{-}Al_2O_3$ and SiO_2 starts at around 500 °C (Fig. 3a). The reduction peak is broad indicating that the reduction of vanadium in the bulk of the oxide is hindered. Over palladium doped catalysts, the main reduction peak appeared shifted to the 80–260 °C (Fig. 3b). At higher temperatures, only small peaks could be discerned even for the catalysts containing bulk vanadia. However, the reduction of the latter catalysts starts and ends at somewhat higher temperatures than reduction of the catalysts covered by vanadia in near to monolayer thickness (Fig. 3b). The H_2 consumption of the Pd/V_2O_5 sample is about five times higher compared to other samples what results in a broad TPR peak. The reduction of samples containing bulk vanadia starts at higher temperature compared to other samples and the maximum of the TPR curve is also at higher temperature, i.e. 163 and 203 °C for $\alpha\text{-}Al_2O_3$ and SiO_2, respectively (Table 2). The total H_2 consumption expressed in H_2/V ratio for each sample varies between 0.90 and 1.15 substantiating that $V^{5+} \rightarrow V^{3+}$ reduction occurred.

Results of catalytic test reactions over different oxide supports are shown in Fig. 4. Note that the conversions and AL selectivities are significantly higher than those shown by Fig. 1 indicating that the reaction follows the mechanism of Wacker

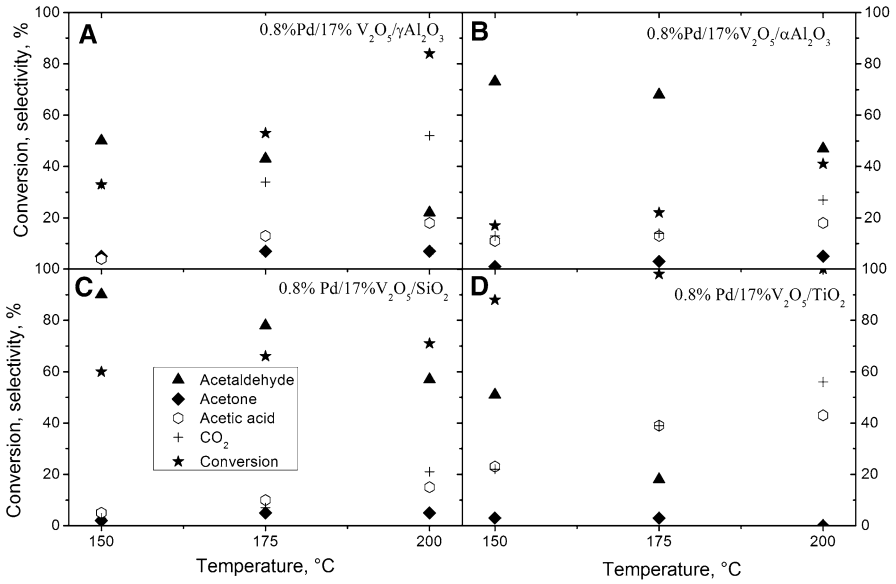

Fig. 4 Catalytic conversion of 3% ethylene/12% oxygen/24% water/He gas mixture as a function of temperature over different catalysts. $m_{cat} \sim 500$ mg, total flow rate 30 cm^3/min

oxidation. The highest yield of partially oxidized products was achieved using Pd/VO_x/SiO_2 catalyst (Fig. 4c). Over Pd/VO_x/α-Al_2O_3 catalyst, the AL selectivity was rather high (45–70%). However, the AL yield was low because the EE conversion was the lowest (20–40%) among the studied catalysts (Fig. 4b). Results represented in Fig. 4d suggest that the titania-supported catalyst has high activity ($\sim$100% conversion), but its selectivity towards partially oxidized products is rather low. The conversion over Pd/VO_x/γ–Al_2O_3 catalyst was similar to that of Pd/VO_x/SiO_2, although its CO_2 selectivity was with about 30% higher than that of the Pd/VO_x/SiO_2 catalyst (cf. Figs. 4a and 4c).

Ethylene conversion and product selectivities are shown as the function of oxygen partial pressure using the 0.8%Pd/V_2O_5 catalyst (Fig. 5b). The selectivities of AA and CO_2 showed a slight increase at the expense of AL selectivity with increasing oxygen concentration in the feed. The EE conversion increased parallel with the increasing selectivities. The reaction was strongly affected by water between 0 and 40 kPa water partial pressures (Fig. 5c). Higher EE conversions and AL selectivities were obtained at higher water partial pressures.

The above results seem to correlate with the structure of supported vanadia. At identical loadings, the structure of the surface-bound vanadia depends on the size and the chemical character of the support surface. Each supported catalyst contains V_2O_5 in a roughly comparable amount (Fig. 2b). However, the surface concentration of the monomeric and polymeric surface vanadia species shows significant difference. The Pd/VO_x active phase over supports of high SSA, like γ–Al_2O_3 and SiO_2, shows high activity in the EE conversion but a significant difference in the selectivity for total oxidation (Figs. 4a and 4c). The main difference is that the silica

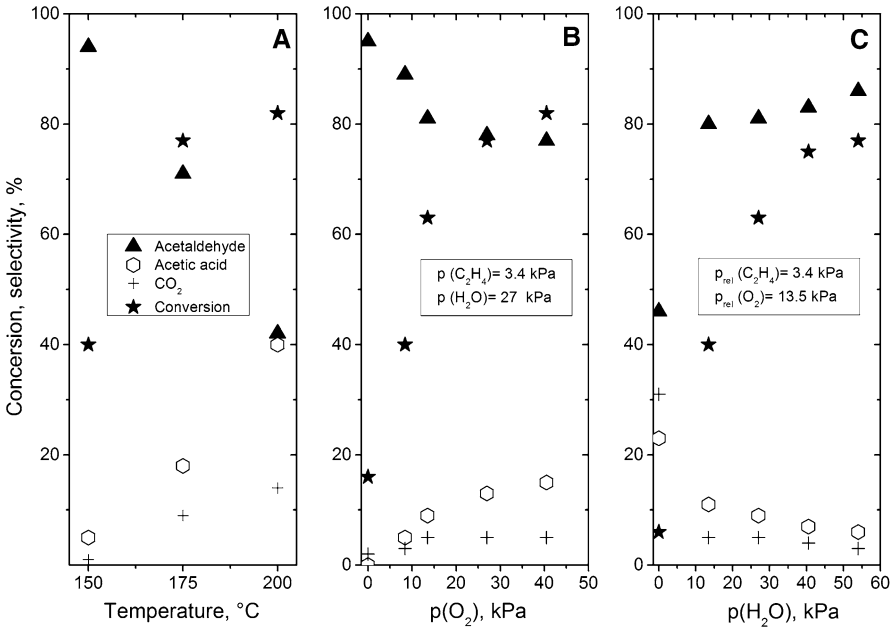

Fig. 5 Catalytic conversion of 3% ethylene/12% oxygen/24% water/He gas mixture over 0.8%Pd/V_2O_5 catalysts as function of **a** temperature, **b** O_2 partial pressure, and **c** water partial pressure. The temperature and the partial pressure dependences were measured at 150 °C, using ~500 and 100 mg of catalyst, respectively. The 100 mg catalyst was diluted to 500 mg by inert γ-Al_2O_3. The total flow rate of the reaction mixture was always 30 cm^3/min

support carries mainly isolated VO_4 surface species, whereas the γ–Al_2O_3 support is rich in polymeric surface vanadia species in close to monolayer thickness. This comparison teaches that polymeric surface vanadia species favor total oxidation but are unfavorable components of the Wacker catalysts. Earlier studies [13, 14, 26] reported that Pd/V_2O_5/TiO_2 catalysts having much lower V_2O_5 content ($\lesssim$10 wt%) than the one used in present study have outstanding activity in Wacker oxidation. The relatively low selectivity of the 0.8%Pd/17%V_2O_5/TiO_2 catalyst for AL and AA formation is in agreement with the finding that at the applied vanadia loading the titania support contains mainly polymeric vanadia species, having high activity in the total oxidation to CO_2 (Fig. 4d). The above results suggest that Wacker activity could be assigned either to isolated VO_4 species and/or to bulk phase V_2O_5 in the catalyst. In order to come to a conclusion, we examined the catalytic performance of non-supported Pd/V_2O_5 catalyst in details (Fig. 5). Fig. 5a shows that 0.8%Pd/V_2O_5 catalyst exhibits catalytic activity that is similar to that of the SiO_2-supported sample. This finding substantiates that selective oxidation activity can be attributed to the presence of redox pair sites generated by Pd, bound either to bulk V_2O_5 or to monomeric VO_4 species, and to the absence of polymeric vanadia species in the catalyst.

The monomeric VO_4 structure on the surface of SiO_2 support is substantially inactive in the oxidation of the primary product AL. The specific surface area of α-

Al_2O_3 support is below 2 m^2/g and impregnation with 17 wt% V_2O_5 results in a surface vanadia coverage value of 68 V/nm^2. It implies that the VO_x structure built on the surface of this support must be very similar to bulk V_2O_5 phase. Still, the UV–vis measurement shows that the supported multilayer of vanadia is different form the bulk V_2O_5. In accordance, the results of the catalytic test reactions (compare Figs. 4b and 5a) manifest that the non-supported sample is more efficient regarding both EE conversion and AL selectivity, especially at lower temperatures.

The γ–Al_2O_3 and TiO_2 supported vanadia can be reduced by H_2 at the lowest temperature (Fig. 3a). The presence of Pd in the catalysts lowers the reduction temperature of vanadia in all the catalysts. The γ–Al_2O_3 and TiO_2-supported vanadia becomes reduced at the lowest temperature (Fig. 3b). The most favorable Wacker catalyst, the SiO_2-supported catalyst containing mainly monomeric VO_4 species, is obviously less reducible than the γ–Al_2O_3 and TiO_2 supported catalysts containing mainly polymeric vanadia species (Fig. 3). The very high reducibility of the polymeric vanadia species can be the reason of the non-selective EE Wacker oxidation property of the γ–Al_2O_3 and TiO_2 supported catalysts.

Conclusions

The oxidation of ethylene by oxygen in the presence of steam was investigated over non-supported, and SiO_2, TiO_2, γ-Al_2O_3, and α-Al_2O_3-supported Pd/V_2O_5 catalysts. The vanadia structures were identified by UV–vis and XRD measurements. Besides some bulk V_2O_5 phase, catalysts contained predominantly either monomeric vanadate-like, VO_4, surface species or bulk V_2O_5 (VO_5/VO_6 polymer) species. It was shown that VO_3 polymeric (metavanadate-like) species are responsible for the ethylene oxidation activity to CO_2 and, as a consequence, for the poor selectivity in the oxidation to acetaldehyde and acetic acid. It was shown that the polymeric VO_3 species was more reducible than the monomeric VO_4 and the bulk V_2O_5 species. Results suggested that the high reducibility of vanadia is responsible for the high activity in the non-selective catalytic oxidation. Better Wacker activity was achieved with the less reducible SiO_2 and α-Al_2O_3-supported Pd/V_2O_5 catalysts than with the very easily reducible TiO_2 and γ-Al_2O_3-supported catalysts. Vanadia over low surface area α-Al_2O_3 and bulk vanadia have similar structures. Nevertheless, the non-supported Pd/V_2O_5 catalyst is more active and selective than the $Pd/V_2O_5/\alpha$-Al_2O_3 catalyst, showing that this support still has adverse effect on the Wacker activity.

Acknowledgement This work was financially supported by the Hungarian Scientific Research Fund, Hungary (OTKA, Contract No. K 100411).

References

1. Arpe HJ (2003) Ethanol. Industrial Organic Chemistry, 4th edn. Wiley-VCH Verlag GmbH & Co. KGaA, Weinheim, pp 193–198
2. Angelici C, Weckhuysen BM, Bruijnincx PCA (2013) Chem Sus Chem 6:1–21

3. Makshina EV, Dusselier M, Janssens W, Degrève J, Jacobs PA, Sels BF (2014) Chem Soc Rev 43:7917–7953
4. Lebedev IE (1930) GB 331482
5. Ostromislenskiy J (1915) J Russ Phys Chem Soc 47:1472–1506
6. Niiyama H, Morii S, Echigoya E (1972) Bull Chem Soc Jpn 45:655–659
7. Han Z, Li X, Zhang M, Liu Z, Gao M (2015) RSC Adv 5:103982–103988
8. Kim TW, Kim JW, Kim SY, Chae HJ, Kim JR, Jeong SY, Kim CU (2015) Chem Eng J 278:217–223
9. Ushikubo T, Kurashige M, Koyanagi T, Ito H, Watanabe Y (2000) Catal Lett 69:83–87
10. Hagemeyer HJ (2002) Acetaldehyde, in Kirk-Othmer encyclopedia of chemical technology, vol 1. Online edn. Wiley, New York, pp 99–114
11. Espeel PH, Tielen MC, Jacobs PA (1991) Chem Commun 10:669–671
12. Mitsudome T, Umetani T, Mori K, Mizugaki T, Ebitani K, Kaneda K (2006) Terahedron Letters 47:1425–1428
13. Stobbe-Kreemers AW, Makkee M, Scholten JJF (1997) Appl Catal A 156:219–238
14. Li M, Shen J (2001) React Kinet Catal Lett 72:263–267
15. Izumi Y, Fujii Y, Urabe K (1984) J Catal 85:284–286
16. Seoane JL, Boutry P, Montarnal R (1980) J Catal 63:182–190
17. Tian H, Ross EI, Wachs IE (2006) J Phys Chem B 110:9593–9600
18. Smidt J, Hafner W, Jira R, Sieber R, Sedlmeier J, Sabel A (1962) Angew Chem Int Ed 1:80–88
19. Mitsudome T, Mizumoto K, Mizugaki T, Jitsukawa K, Kaneda K (2010) Angew Chem 122:1260–1262
20. Wachs IE, Weckhuysen BM (1997) Appl Catal A 157:67–90
21. Bond GC, Tahir SF (1991) Appl Catal 71:1–31
22. Deo G, Wachs IE (1994) J Catal 146:323–334
23. Gao X, Wachs IE (2000) J Phys Chem B 104:1261–1268
24. Zhang C, Li Y, Wang Y, He H (2014) Environ Sci Technol 48:5816–5822
25. Van der Heide E, Zwinkels M, Gerritsen A, Scholten J (1992) Appl Catal A 86:181–198
26. Barthos R, Hegyessy A, Novodarszki G, Pászti Z, Valyon J (2016) Appl Catal A. doi:10.1016/j.apcata.2016.10.024